Tellus (1996), 48A, 368–382
Printed in UK – all rights reserved

TELLUS
ISSN 0280–6495

Validity of similarity relations over the Gulf Stream

By NEERAJA C. REDDY and SETHU RAMAN*, *Department of Marine, Earth and Atmospheric Sciences, North Carolina State University, Raleigh, NC 27695–8208, USA*

(Manuscript received 2 August 1995; in final form 3 November 1995)

ABSTRACT

Observations obtained from aircraft, buoys, ships and vertical soundings made on 9, 10 and 22 February, 1986 during the Genesis of Atlantic Lows Experiment (GALE) are used to study the mean marine boundary-layer (MBL) structure over the cold coastal waters and the warm Gulf Stream. Different synoptic conditions prevailed on each day. The synoptic setting was characterized by prestorm conditions on 9 February and meso-low development on 10 and again on 22 February. Two convergence zones, one near the Gulf Stream and the other close to the coast were observed on both the days of cyclogenesis causing different stability conditions in the MBL near the coast and the Gulf Stream. The boundary-layer on 9 February was however well mixed . Temperature and humidity variances during prestorm conditions (9 February) generally followed the free convection relations. But on 10 and 22 February, in the presence of a meso-low, similarity relations do not appear to be valid for temperature and humidity variances and fluxes.

1. Introduction

Large horizontal temperature gradients occur during winters off the coast of the Carolinas because of the existence of the Gulf Stream with a sea surface temperature of about 25°C. Coastal waters, on the other hand, have surface temperatures typically in the range of 6 to 9°C. Land surface on the other hand can have surface temperatures varying from 0 to 10°C depending on the time of the day. Such large variations in the surface temperatures cause sharp gradients in surface heat fluxes which in turn cause mesoscale variations in boundary layer structure and local convergences.

Explosive east coast cyclones occur most frequently in winters near regions of strong sea surface temperature (SST) gradients (Sanders and Gyakum 1980). Occurrence of large surface heat and moisture fluxes in the vicinity of the Gulf Stream can have a significant effect on storm development. The fluxes increase the buoyancy of the air in the boundary-layer, and enhance coastal frontogenesis. Coastal frontogenesis (Bosart et al., 1972; Bosart 1975, 1981) and coastal cyclogenesis (Kocin and Uccellini 1985a, b; Bosart 1981; Sanders and Gyakum 1980; Sanders 1986) in this region have been studied extensively. However, even though it is generally acknowledged that the thermodynamic forcing of the Gulf Stream can play a role in the dynamics of both these phenomena, until recently very little effort was devoted to the understanding the marine boundary-layer (MBL) processes. Numerical studies (Kuo et al., 1991; Anthes et al., 1983; Atlas 1987; Uccellini et al., 1987) have indicated the importance of the MBL in causing rapidly deepening cyclones. There have been several observational studies of the marine boundary-layer structure during cold air outbreaks (Wayland and Raman, 1989; Rogers, 1989;, Chou et al., 1986), but very few in disturbed conditions.

Recently, the Genesis of Atlantic Lows Experiment (GALE) was conducted in the mid-Atlantic coastal region of the United States. The

* Corresponding author.

GALE field study, carried out between 15 January, 1986 and 15 March, 1986, was one of the largest weather experiments conducted in the United States. Aircraft, radars, sounding systems, satellites, ships and buoys were utilized to monitor changes in atmospheric/oceanic conditions. The main purpose of this experiment was to determine the processes involved in the development of extratropical cyclones offshore of the Carolinas. The objective was also to study several mesoscale phenomena such as cold-air damming, coastal fronts, cloud and rain bands and cold-air outbreaks, and to investigate their relative contributions to the cyclogenesis events. Design of the experiment is discussed by Dirks et al., (1988) and a description of the planetary boundary-layer (PBL) observation systems is given by Raman and Riordan (1988).

The main objective of this paper is to compare the boundary-layer mean and turbulence structure during pre-storm conditions with those observed during cyclogenesis conditions. Emphasis in this paper is placed on understanding the turbulence statistics and the validity of similarity relations in the marine boundary-layer during disturbed and undisturbed conditions over the western Atlantic Ocean. For this purpose, observations collected on 9, 10 and 22 February 1986 are used. Synoptic flow on 9 February 1986 was essentially a "prestorm" condition with northeasterly flow. On both 10 and 22 February, a meso-low developed near the western edge of the Gulf Stream.

2. Observations and methodology

2.1. Observations

A variety of National Weather Service (NWS) and GALE surface and upper-air data are used in this study. The primary datasets used in this paper are those from the two NCAR research aircraft, King Air and Electra. The upper air sounding data were obtained from Cross-Chain Loran Atmospheric Sounding System (CLASS), rawinsondes, mini-radiosondes, and Omega dropwindsondes.

The special GALE surface data were obtained from 51 Portable-Automated-Mesonet (PAM) II sites, eight instrumented GALE research buoys, NOAA and one oceanographic research vessel, R/V Cape Hatteras. The sea surface temperature (SST) field used in this study was derived from the NOAA-9 infrared imagery. This 1.1 km high resolution imagery helped in resolving the strong sea surface temperature gradients (SST) associated with the western edge of the Gulf Stream. Observations of cloud type and structure and cloud top heights were obtained from reports by observers onboard the aircraft.

2.2. Research aircraft flight plan

9 February and 10 February. The flight track on 9 February is shown in Fig. 1. A high resolution Sea surface temperature (SST) distribution on 9 and 10 February was not available due to the presence of clouds. However, high resolution (1.1 km) SST on 8 February (Fig. 2) indicates meandering of the Gulf Stream leading to the formation of filaments offshore of the Carolinas. The Gulf Stream position was obtained from the report provided by the NOAA/AOML (Atlantic Oceanographical Meteorological Laboratory) at 1800 UTC on 10 February and is shown in Fig. 1. The solid line indicates the maximum sea surface temperature contour of 22°C defining the western edge of the Gulf Stream. The dashed line indicates the eastern edge of the Gulf Stream. Positions A and B indicate regions where vertical profiles of mean and turbulence structures were obtained by King Air aircraft on 9 February (Figure 3a). A level-wing descent from 1500 m was first flown at

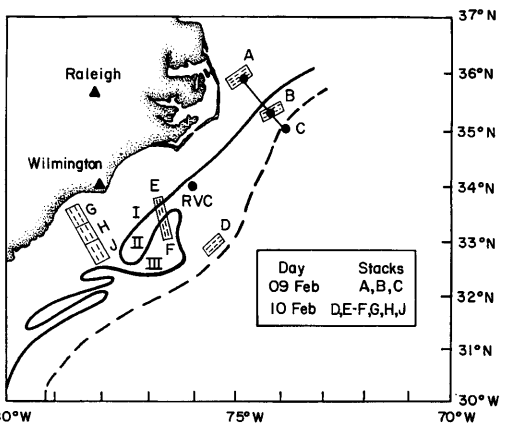

Fig. 1. King air and Electra flight tracks on 9 and 10 February. Locations A, B and C were taken on 9 February; and D, E–F, G, H, and J were flown on 10 February, respectively.

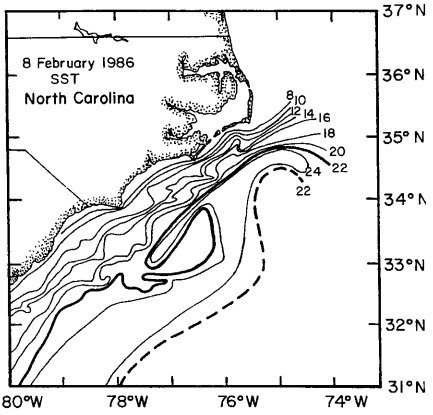

Fig. 2. SST distribution on 8 February.

A (35.9°N, 75°W) at approximately 1630 UTC over the cold shelf waters (SST = 12–14°C) to obtain vertical boundary-layer structure. The aircraft then proceeded at 40 m altitude from A to a location C (35.6°N, 73.8°W) east of the Gulf Stream core (SST = 20°C) for a distance of 120km to map low level winds, temperatures and fluxes. Observations from this low level transect are discussed later. The flight then made a return transect from C to location B (35.8°N, 74.25°W), over the Gulf Stream (SST = 24°C) at 40 m altitude. At B a vertical stack consisting of a series of tracks were flown at five altitudes in the sub cloud layer. One level-flight was also made above cloud top in the free atmosphere.

The flight from B to A was approximately at 400 m altitude (roughly 45 km between A and B). A vertical stack was flown at A (1830 UTC) similar to that at B. Upon completion of the last leg at A (altitude of 2000 m), a level-wing descent was flown at 1850 UTC to obtain vertical boundary-layer structure at location A.

The flight plan for the NCAR King Air and Electra aircraft on 10 February is also shown in Fig. 1. One stack (G to J) was flown by Electra aircraft and two stacks at D (over the Gulf Stream) and E to F (across the Gulf Stream filament) were taken by the King Air aircraft (Figure 3b).

On 10 February, the King Air departed from Raleigh at 1200 UTC. A level wing descent from 1500 m was first flown at D (32.8°N, 75.8°W) over the Gulf Stream waters (SST = 24°C) at 1300 UTC. A vertical stack consisting of a series of level 300–400 s legs (23.1 km–30.8km in length at an aircraft speed of 77 m s^{-1}) at four altitudes in the subcloud layer was flown. A vertical stack consisting of a series of level 300–720 s (23.1 km – 55.5 km in distance at an aircraft speed of 77 m s^{-1}) at 4 altitudes in the subcloud layer was flown at E to F (33°N, 77°W). This stack was flown perpendicular to a Gulf Stream "filament", a tongue like extrusion of the Gulf Stream warm waters into cold mid shelf waters (see Figs. 1, 2). High resolution (1.1 km) SST on 8 February (Fig. 2) indicates meandering of the Gulf Stream leading to the formation of filaments offshore of the Carolinas. The SST distribution on 10 February (Fig. 1) indicated that the filaments were quasi-stationary during this period. The filament was oriented NE-SW approximately parallel to the Gulf Stream. The SST varied from 18°C over mid-shelf to 24°C over the filament to 19°C over the cold core waters between the filament and the western edge of the Gulf Stream.

The NCAR Electra aircraft departed from Raleigh at 1630 UTC on 10 February and took vertical profilings along the M-Surfaces over land. At about 1800 UTC, 7 vertical cross sections across this frontal feature were flown at altitudes of 50 m, 90 m, 150 m, 200 m, 320 m, 630 m and 1200 m (SST = 9–23°C and location = 330°N, 77°W) for 12 to 20 minutes (100 km–140 km) at an aircraft speed of 110 m s^{-1}. The length of each leg flown by Electra aircraft is divided into 3 to 4 segments (approximate duration of 5 min). First segment represents near shore waters (G) with SST between 10°C and 13°C, the second represents near shore shelf waters (H) with SST between 13°C and 16°C, the third represents mid-shelf waters (H-J) with SST between 16°C and 19°C and the fourth represents the transition region towards the Gulf Stream waters (J) with SST between 19°C and 22°C (between the mid-shelf waters and the warm Gulf Stream waters).

22 February. The flight track of National Center for Atmospheric Research (NCAR) King Air on 22 February offshore of Carolinas is given in Fig. 3 along with the high resolution (1.1 km) sea surface temperature (SST) analysis of 21 February, 1986. Due to the presence of clouds offshore on 22 February, SST analysis on 21 February was used (the closest date on which the cloud activity was less offshore). This SST data was obtained from NOAA-9 satellite. Derived from satellite, this

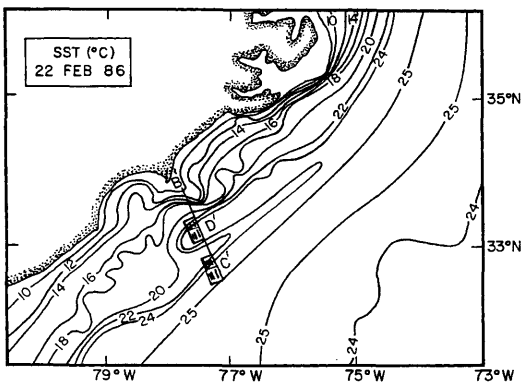

Fig. 3. King Air flight tracks on 22 February.

analysis represents a composite of two to three days of imagery in order to eliminate cloud effects.

Near shore waters are cold, especially north of Cape Hatteras and along the coast. A strong baroclinic zone exists off Carolinas. An oceanic feature called filament, which is a tongue-like extrusion of the Gulf Stream warm waters into cold shelf waters is aligned almost parallel to the east coast and is about 60–70 km far from the coast. A strong oceanic thermal gradient, generally known as the mod shelf front (located at D′) is distinguishable from the west wall of the Gulf Stream (located at C′).

The initial flight plans of King Air on 22 February were to obtain flux profiles over the mid shelf front and the Gulf Stream core during a period of southwesterly flow and to investigate the coastal front structure. The King Air flight took a level wing descent at B′ (33.6°N, 77.8°W) from 3000 over the cold shelf waters (SST = 110C) at 1745 UTC on 22 February (Figure 5). Then the flight proceeded from B′ to C′ (32.8°N, 77.4°W) at about 40 m altitude. This low level transect is about 160 km long (Fig. 3). A vertical stack consisting of a series of level 300–400 s legs (23.1–31 km in length at an aircraft speed of 77 m s^{-1}) at six altitudes (30 m, 100 m, 150 m, 250 m, 350 m and 1100 m). Another low-level transect was made by King Air from C′ to D′ at 40 m altitude. A vertical stack consisting of a series of level 300 s to 400 s at four altitudes (40 m, 300 m, 150 m, 2000 m) was flown at 1900 UTC. A level wing ascent from 150 m to 2000 m was made at D′ at approximately 1930 UTC.

3. Mesoscale analysis

Mesoscale surface analysis offshore on 9 February (not shown) indicated weak (1–2 m s^{-1}) northerly winds along the coast. But strong (10 m s^{-1}) northeasterly winds were present over the Gulf Stream. The mesoscale surface analysis at 1700 UTC 10 February is shown in Fig. 4a. The horizontal divergence values shown in Figure 4b are estimated using the mean wind components (u and v) interpolated on to 25 km grid points. The values of $\partial u/\partial x$ and $\partial v/\partial y$ are then estimated using finite differencing method. This analysis indicates two low level mesoscale convergence zones (solid lines in Fig. 4b), one near the western edge of the Gulf Stream (7.8×10^{-5} s^{-1}) and the other near the coastal waters

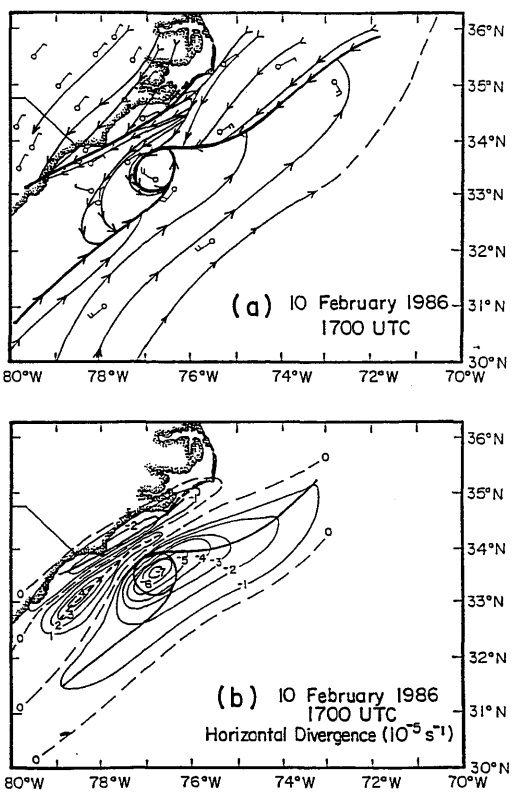

Fig. 4. Mesoscale analysis on 10 February at 17 UTC. (a) Stream line analysis. Heavy solid lines indicate the confluence zones. (b) Contours of estimated convergence. Heavy solid lines indicate the convergence zones and heavy dashed line indicate the divergence zone.

(3.4×10^{-5} s^{-1}) offshore of Wilmington (G) with a divergence zone (3.1×10^{-5} s^{-1}) in between (location H, solid dashed line). Wind speeds increased by a factor of two from 4.8 m s^{-1} over mid-shelf waters to 9.5 m s^{-1} at the western edge of the Gulf Stream. A meso-low is located at 33°N, 77°W (location E–F) on 10 February at 17 UTC (Figure 4a). Similar convergence/divergence zones were also observed by Riordan (1990) and Holt and Raman (1990) for other days during coastal frontogenesis.

Mesoscale surface analysis from the PAM network, ships, and buoys for 18 UTC on 22 February in the region of the cold front offshore is shown in Fig. 5. At 06UTC (not shown) on 22 February, moderate northeasterly flow (5 m s^{-1}) occurred along the coast from Cape Hatteras (35.30°N; 75.50°W) to Wilmington, but the south-southwesterly flow in the vicinity of Charleston, SC (32.90°N, 800°W). Visible satellite imagery at 06UTC (not shown) however indicated little organized cloud activity in this region, suggesting that if a cold front existed at this time, convective activity was weak. Similar conditions prevailed up to 12 UTC.

The line connecting B′, D′ and C′ indicate the King Air low level transect at approximately 18 UTC (Fig. 5a). It is difficult to pinpoint the frontal location from the aircraft data due to the development of a cyclone offshore of Wilmington. An interesting feature at 18 UTC revealed by satellite observations is the presence of organized cloud activity along the coastal front (not shown). Stream line analysis (Fig. 5b) and satellite imagery confirm the development of a meso-low offshore between cyclonic rotation 17UTC and 21 UTC (32.8°N, 77.5°W). This strong circulation was not evident earlier at 12 UTC. This meso-low formed near the western edge of the Gulf Stream in the region of the NCAR King Air boundary layer flight. When SST are superimposed on the mesoscale analysis (Figs. 3 and 5), the surface cyclone is located over the Gulf Stream. Similar development of a meso-low offshore over the Gulf Stream filament was also observed by Reddy and Raman (1994).

4. Turbulent structure of the marine boundary-layer

High-rate (or 20 samples/s, sps) data were utilized. In analyzing the turbulent structure of the MBL, surface fluxes and other turbulent statistical that characterize the turbulent structure of the boundary-layer were estimated. Appropriate scaling parameters such as the surface friction velocity (u_*), the convective velocity scale (w_*), the convective temperature scale (θ_*), the convective humidity scale (q_*), convective time scale (t_*), and the Monin-Obukhov length (L) were determined. Aircraft flux data collected at lowest flight levels were linearly extrapolated to the surface to get the surface fluxes using eqs (1) and (2). Table 1summarizes the above values at various heights and locations sampled by the King Air and Electra aircraft. Also given in Table 1 are surface sensible (H) and latent (E) heat fluxes:

$$H = \rho c_p (\overline{w'\theta'})_0 , \quad (1)$$

$$E = \rho L_v (\overline{w'q'})_0 , \quad (2)$$

where, r is density, c_p is specific heat of air (1004 J kg^{-1} K^{-1}) and L_v is the latent heat of vaporization (2.45×106 J kg^{-1}). Total heat flux is the sum of sensible and latent heat fluxes. To estimate these heat fluxes, bulk aerodynamic method was used with ship. Fluxes from aircraft data are based on eddy correlation.

On 9 February, a SST difference of 14°C was observed between the coastal waters and the Gulf Stream (Table 1). The boundary-layer height (h) over the Gulf Stream increased by about 50% (600 m). Surface total heat fluxes over coastal waters are about 60 W m^{-2} and increased to 270 W m^{-2} over the Gulf Stream. The surface friction velocity increased by a factor of 2.2 over the Gulf Stream (0.45) as compared to coastal waters (0.2) indicating an increased wind speed over the Gulf Stream. Convective velocity scale (w_*) increased by almost a factor of two due to the increase in the sensible heat fluxes and the height of the boundary-layer over the Gulf Stream. Boundary-layer was convective over both the locations (A and B) as indicated by the Monin Obhukov length (Table 1).

On 10 February, the SST difference from J (mid shelf waters, MS) to D (Gulf Stream) is only about 4°C. However, SST gradient from cold shelf waters to Gulf Stream waters is about 16°C. The boundary-layer height increased by about 75% and the total heat fluxes increased by a factor of about seven over the Gulf Stream as compared to location J. Small heat fluxes over the location J is

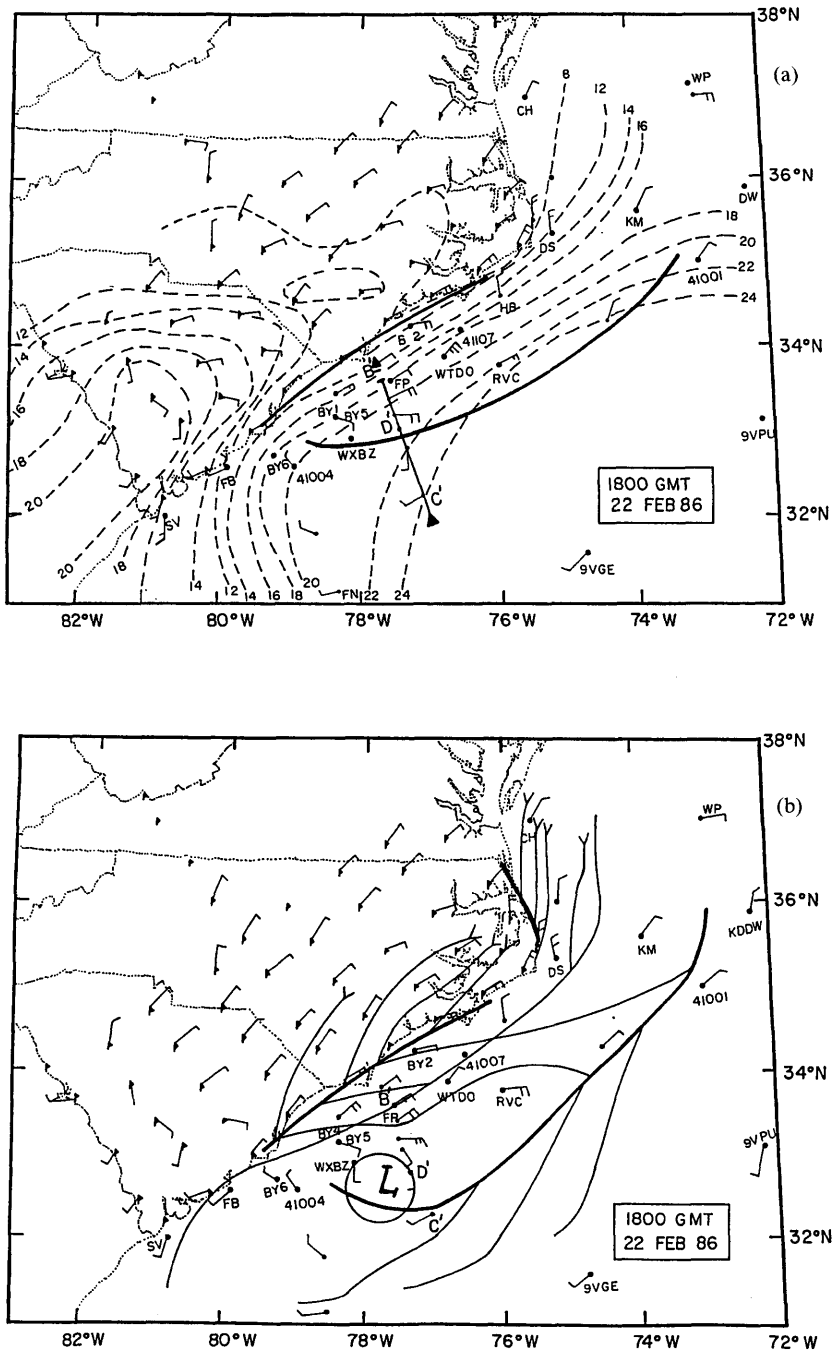

Fig. 5. (a) Mesoscale analysis on 22 February at 18 UTC and (b) streamline analysis. Heavy solid lines indicate the confluence zones.

Table 1. *Boundary layer fluxes and parameters on 9, 10 and 22 February*

Region	A CS	B GS	D GS	C′ GS	D′ MS
Time (UTC)	1830	1700	1300	1830	1900
SST (°C)	10.0	24.0	24.0	25.0	20.0
h	400	600	700	1100	600
w_*	0.63	1.45	1.15	1.51	1.01
u_*	0.20	0.45	0.37	0.53	0.25
θ_*	0.04	0.10	0.05	0.07	0.05
q_*	0.01	0.02	0.05	0.08	0.03
$(\overline{w\theta_v})_s$	0.024	0.15	0.06	0.09	0.06
$(\overline{w'q'})_s$	0.006	0.028	0.056	0.10	0.03
$(\overline{u'w'})_s$	−0.03	0.09	−0.02	−0.12	−0.02
$(\overline{v'w'})_s$	0.02	0.18	−0.11	−0.28	−0.06
$-L$ (m)	24	45	63	123	18
$-h/L$	12	18	12	9	33
H (W m^{-2})	30	185	75	100	76
E (W m^{-2})	28	85	170	270	85

CS and GS indicate cold coastal shelf waters and Gulf Stream waters, respectively. Data at A and B was measured on 9 February and D was measured on 10 February. Units are in SI. C′ and D′ were measured on 22 February 1986.

because of its proximity to the divergence zone. Winds are very light in this region (about 3 m s^{-1}). Friction velocity increased by about 50% but the convective velocity increased by a factor of two over the Gulf Stream. The boundary layer over coastal shelf waters is stable.

On 22 February similar conditions prevailed as those on 10 February. Conditions at C′ are convective whereas D′ is located in a disturbed weather conditions. SST gradient from coastal waters to the Gulf Stream waters are about 15°C. As expected, boundary layer height increased from D (600 m) to C (1100 m) by about 90%. Surface fluxes of total heat increased by a factor of three, convective velocity increased by a factor of 1.5 and surface friction velocity scale increased by a factor of 2 over the Gulf Stream as compared to mid shelf waters. The increase in these turbulent parameters from mid-shelf to Gulf Stream waters are primarily due to the effects of the warm Gulf Stream waters and the developing cyclone in that region.

A comparison of turbulence parameters (boundary layer height, h and vertical velocity, w_*) from prestorm (9 February) to disturbed conditions (10 February and 22 February) indicates the boundary layer is highly convective over the Gulf Stream during disturbed weather conditions. The latent heat fluxes also increased by 3–5 times over the Gulf Stream from prestorm conditions to meso-low development. Similar increase in surface temperature and humidity variances over the Gulf Stream can be clearly seen from Table 1.

4.1. *Spatial variation of the surface turbulent fluxes*

Several investigators (Kuo et al., 1991; Anthes et al., 1983; Warner et al., 1990; etc.) showed that surface heat fluxes have a substantial influence on rapidly deepening cyclones, particularly over the Gulf Stream. In this section, distribution of the surface heat fluxes during a meso-low development are discussed. The contours of total heat fluxes (sensible + latent) on 9, 10 and 22 February are shown in Figs. 6, 8 and 9 respectively.

The total heat flux (W m^{-2}) increased uniformly from cold shelf waters to the Gulf Stream on both days as expected. On 9 February, the total heat flux near the Gulf Stream edge was about 200 W m^{-2} (Fig. 6). However, the aircraft data near the Cape Hatteras indicates a total heat flux of about 340 W m^{-2} over the Gulf Stream. Increased heat flux over this region could be due to the upwelling waters. As can be clearly seen from Fig. 7a, SST

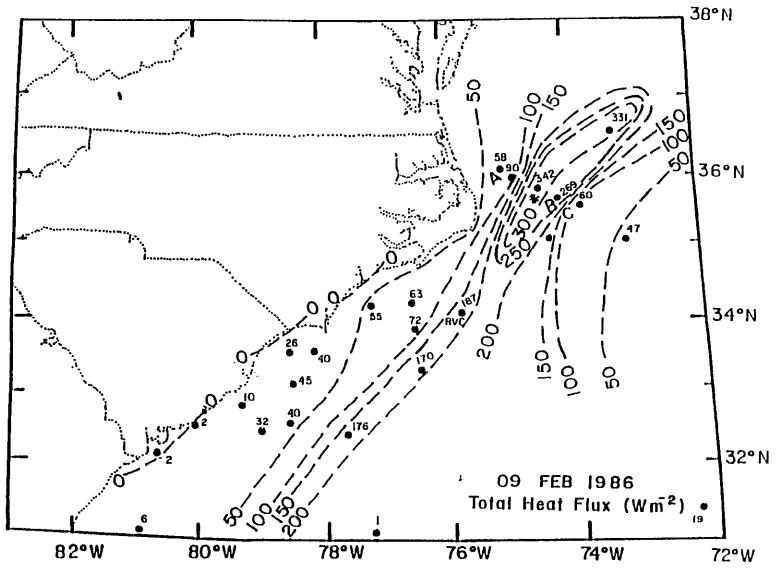

Fig. 6. Spatial variation of total surface turbulent heat fluxes on 9 February obtained from buoy, ships and King Air aircraft data over the observation region. Locations A, B and C are as shown in Fig. 1.

are cooler (12°C) close to the edge of the Gulf Stream and increased to 24°C over the Gulf Stream. The cooler currents from the north are entrained by the Gulf Stream. The upwelling near the Gulf Stream edge is due to the increased winds caused by the increased heat flux gradient. As the cooler air from the upwelling region crossed the Gulf Stream, a large increase in the wind speed and the vertical temperature gradient could have caused a large heat flux. The low level aircraft stack from A to C on 9 February (Fig. 7) indicates an air temperature of about 10°C (SST = 12°C) and 14°C (SST = 24°C). These strong vertical gradients in temperature over the Gulf Stream could have caused the large sensible heat flux. The heat fluxes again decreased towards the Sargaso sea region to values as low as 50 W m^{-2}. As can be seen from Table 1, Sensible heat flux at location B is 185 W m^{-2} as compared to latent heat flux of 85 W m^{-2}. The large sensible heat flux in this region could be driven by strong horizontal surface temperature gradients (0.125°C km^{-1}). The sounding near the Cape Hatteras (HAT) indicates a relative humidity of 50–60% (absolute humidity of 6.8 g m^{-3}) as compared to a relative humidity of 55–70% (absolute humidity of 8.8 g m^{-3}) within the MBL over the Gulf Stream. The moisture profiles (not shown) over coastal waters and Gulf Stream waters indicate a weak moistening. These weak gradients in moisture in vertical and horizontal resulted in weak latent heat fluxes over the Gulf Stream.

The spatial variation of fluxes on 10 February is shown in Fig. 8. As expected, horizontal distribution of the heat fluxes are quite similar to that of the SST, particularly over the filament. The horizontal SST gradients on 10 February are about 0.0621°C km^{-1}. The region of negative heat fluxes close to the coast indicate stable conditions. The heat flux values are of the order of 300 W m^{-2} over the Gulf Stream in the region of meso-low. The latent heat flux gradient weakened considerably westward over the cold shelf waters where a divergent flow was present. A comparison of heat flux values at RVC on both days indicates that the values increased from 187 W m^{-2} on 9 February to a value of 460 W m^{-2} on 10 February during the formation of a meso-low (centered at 33°N, 77°W) mainly due to an increase in the wind speed and evaporation over this region.

Fig. 9 shows the spatial distribution of total heat flux in the region of the offshore meso-low development at 1800 UTC 22 February based on aircraft and available ship and buoy observations. The horizontal SST gradients offshore of Carolinas are about 0.072°C km^{-1}. Fluxes from

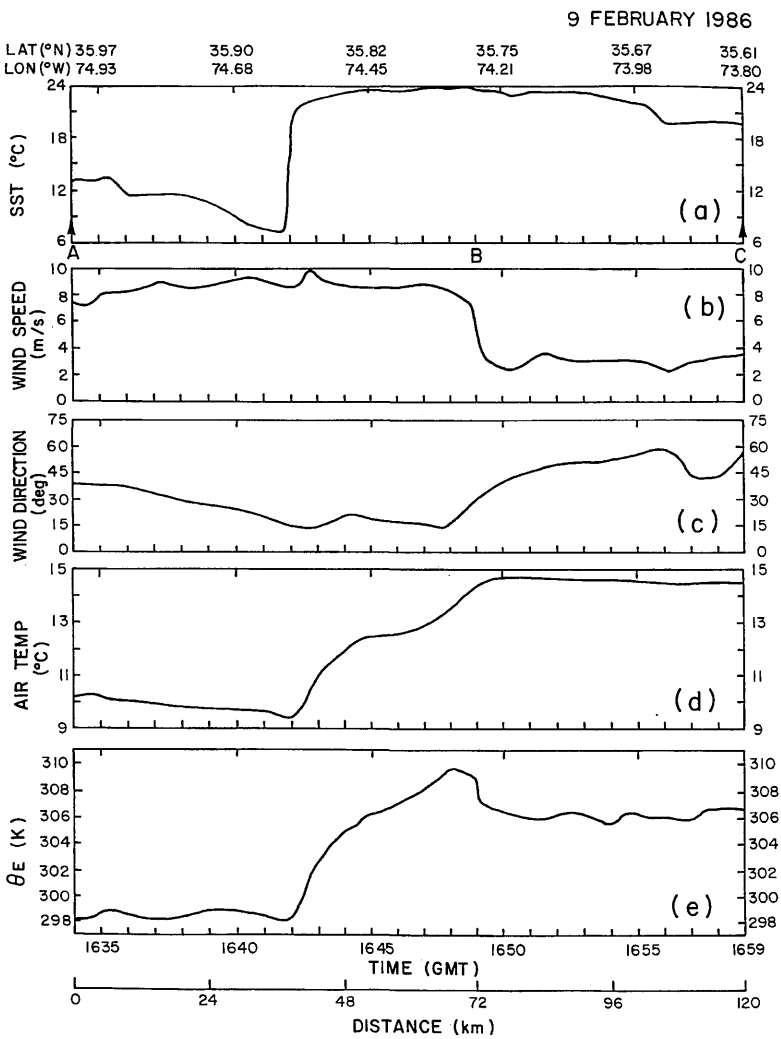

Fig. 7. Spatial variation of (a) SST, (b) wind speed, (c) wind direction, (d) air temperature and (e) equivalent potential temperature along the aircraft low-level stack from A to C on 9 February 1986.

the ship were estimated using the bulk aerodynamic method (Friehe and Schmitt 1976). The local maximum of total heat flux (sensible + latent heat flux) occurs over the Gulf Stream near C′ (380 W m^{-2}) with a strong gradient at the western edge of the Gulf Stream. The total heat flux over mid-shelf waters is 150 W m^{-2} and negative heat fluxes occurred over cold waters (B′). The negative heat fluxes at B′ are due to stable conditions prevailing in that region. However, latent heat flux gradient decreased westward towards the region of difluence (just west of D′) and then increased towards the Gulf Stream.

The data collected in the region offshore of Cape Fear, North Carolina by Raman et al. (1986), encountered SST gradients of about 0.0679°C km^{-1} with highly convective conditions offshore over the Gulf Stream, with measured total heat flux of about 600 W m^{-2}. The air-sea temperature difference encountered during this study was about 10–15°C. Holt and Raman (1990) during an offshore redevelopment of a cyclone on

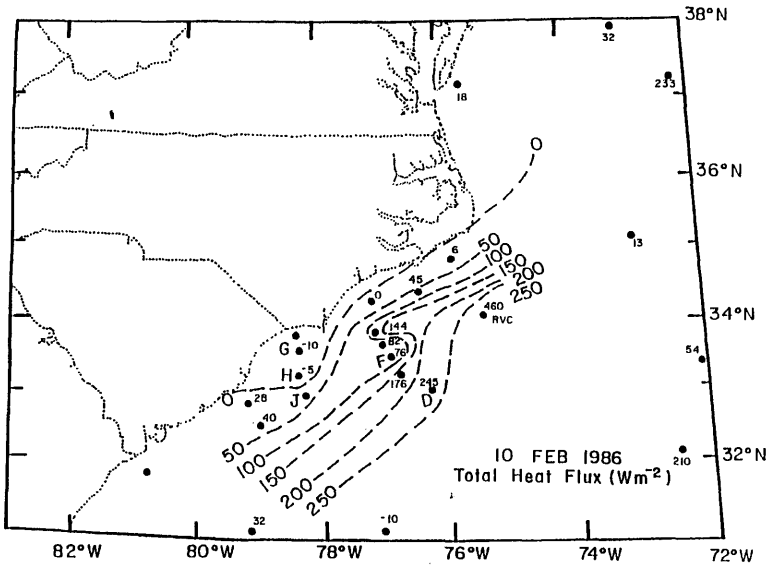

Fig. 8. Spatial variation of total surface turbulent heat fluxes on 10 February obtained from buoy, ships and King Air aircraft data over the observation region. Locations D, E–F, G, H and J are as shown in Fig. 1.

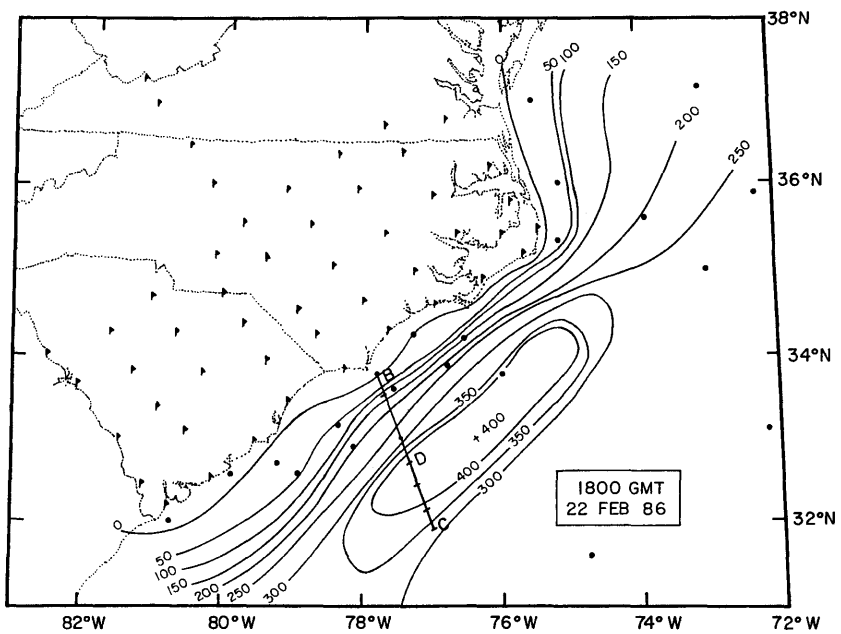

Fig. 9. Spatial variation of total surface turbulent heat fluxes on 22 February obtained from buoy, ships and King Air aircraft data over the observation region. Locations C′ and D′ are as shown in Fig. 3.

24 February 1986 (2 days after the present study) observed SST gradients of about 0.0558°C km^{-1}. The estimated values of total heat flux of Holt and Raman (1990) are about 300 W m^{-2} with similar atmospheric conditions and SST gradients offshore which are present on 22 February 1986. The increased values of total heat fluxes on 22 February as compared to Holt and Raman (1990) could be due to slightly increased values of air-sea temperature difference, strong winds and SST gradients offshore which could have caused increased convection in this region.

During MASEX (Chou et al., 1986) which was conducted offshore of New Jersey and Delaware (35–41°N, 76–69°W) about 160 km north of the GALE region, encountered SST variation of up to 7°C, resulting in the largest SST gradient being 0.057°C km^{-1}. However, the MASEX total heat flux values are half of those observed during GALE because, this region did not encounter the extremely warm currents of the Gulf Stream and thus the heat fluxes are considerably less. Thus, the flux values are consistent with the previous experiments.

The large fluxes over the Gulf Stream are due to the large air-sea temperature differences and strong winds prevailing in this region caused due to a developing cyclone. In response to these large fluxes boundary layer height increased appreciable offshore (Table 1).

4.2. *Validity of similarity relations*

In this section, the profiles of normalized horizontal and vertical velocity, temperature and humidity variances and fluxes are discussed. It will be of interest to determine as to whether similarity relations are valid during disturbed weather conditions (occurred on 10 and 22 February) such as the ones studied here. The averaging time used in this part of the analysis is approximately 5 min, which contains 6000 data points. Sharp SST gradients in this location preclude longer averaging times.

Temperature and humidity variances of the turbulent fluctuations. Profiles of the normalized variances of the fluctuations of temperature and humidity measured on 9, 10 and 22 February at different locations are shown in Figs. 10, 11, along with the local free convection curve (solid linear line) of Wyngaard et al (1971). Variances

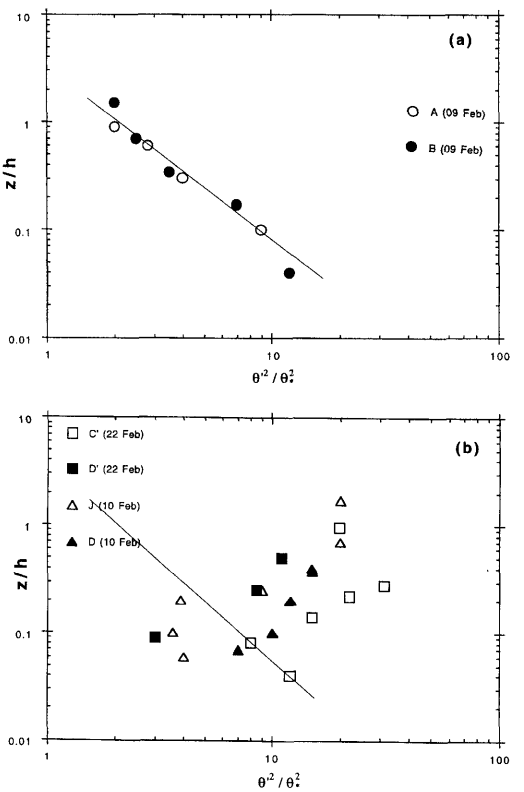

Fig. 10. Normalized potential temperature variances on (a) 9 February and (b) 10 and 22 February. Solid diagonal lines are free convection predictions. Locations A, B, J and D are as shown in Fig. 1 and C′ and D′ are as shown in Fig. 3.

were normalized using surface layer temperature and humidity scales obtained from surface turbulent fluxes. In mixed layer scales, free convection form in the atmospheric boundary-layer (ABL) is generally found to be,

$$\frac{\overline{\theta^2}}{\theta_*^2} = \frac{\overline{q^2}}{q_*^2} = 1.8\,(z/h)^{-2/3}, \qquad (3)$$

where h is the boundary-layer height.

Circles in Fig. 10a indicate the data collected on 9 February over the colder waters at A, and the warmer waters at B (for location of A and B see Fig 1). Normalized temperature variances $\overline{\theta^2}/\theta_*^2$ on 9 February (Fig. 10a) confirm fairly well with the free convection curve. But on 10 and 22 February when a mesoscale circulation was developing, the temperature variances (Fig. 10b)

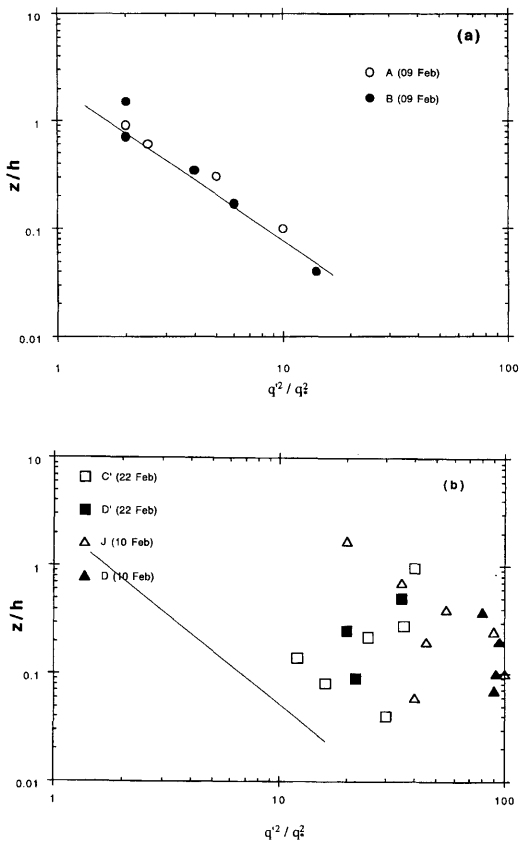

Fig. 11. Normalized humidity variances on (a) 9 February and (b) 10 and 22 February. Solid diagonal lines are free convection predictions. Locations A, B, J and D are as shown in Fig. 1, and C′ and D′ are as shown in Fig. 3.

did not follow the free convection relations. Similar result can be seen from normalized humidity variances $\overline{q^2}/q_*^2$, which are in reasonable agreement with the free convection predictions on 9 February (Fig. 11a). Normalized humidity variances on both days (10 and 22 February, Fig. 11b) are much higher than the local free convection predictions and are increasing with height. A large scatter in the normalized variances on 10 and 22 February can be seen in Fig. 10b and 11b. This is believed to be due to the strong circulation associated with the meso-low and its inherent non-stationarity. Similar conditions were also observed during 24 February 1986 offshore cyclone development (Holt and Raman, 1990).

Profiles of normalized horizontal velocity variance $[(\overline{u'^2}+\overline{v'^2})/2]$ and vertical velocity on 9, 10 and 22 February are shown in Figs. 12 and 13 respectively. The variances were normalized by the square of convective velocity, w_*. Observations are from stacks A and B on 9 February, stacks D and J on 10 February and stacks B′ and C′ on 22 February. The normalized horizontal variance on 9 February (Fig. 12a), have a range of values between 0.4 and 0.6 at both the stacks similar to the values obtained by of Holt and Raman (1990). These normalized values are almost constant with height. But on 10 February and 22 February (Fig. 12b), vertical distribution of normalized horizontal variance is quite different over the Gulf Stream as compared to the coastal waters. Over the coastal region, they have a near constant value

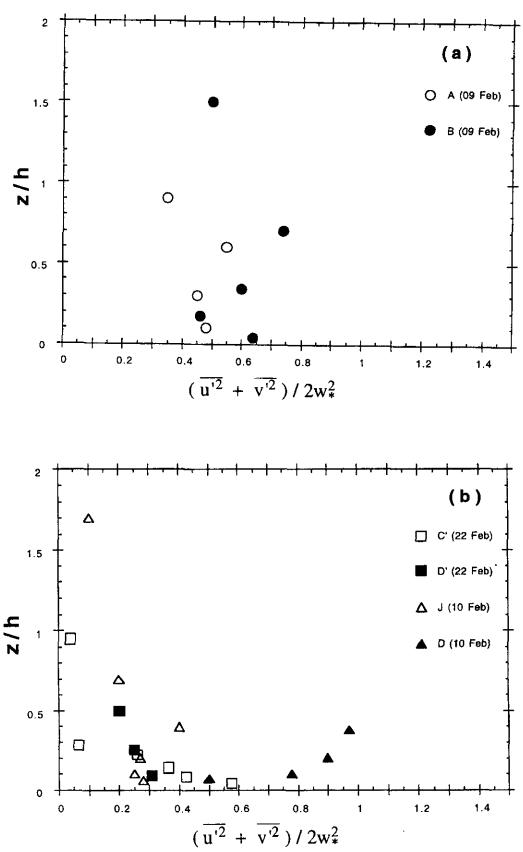

Fig. 12. Normalized horizontal velocity variances on (a) 9 February and (b) 10 and 22 February. Solid diagonal lines are free convection predictions. Locations A, B, J and D are as shown in Fig. 1, and C′ and D′ are as shown in Fig. 3.

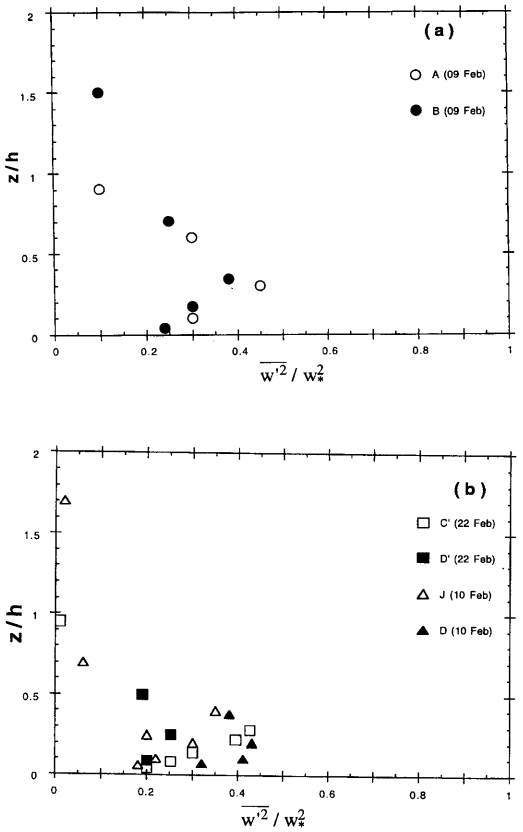

Fig. 13. Normalized vertical velocity variances on (a) 9 February and (b) 10 and 22 February. Solid diagonal lines are free convection predictions. Locations A, B, J and D are as shown in Fig. 1 and C′ and D′ are as shown in Fig. 3.

of about 0.3, about 25% less than the previous day. Recall the MBL is stable just east of this region on 10 February. Over the Gulf Stream where MBL was convective in addition to having a strong mesoscale circulation, normalized horizontal variance values are quite large (0.8 to 0.9). Similar increase in normalized horizontal variance values on 22 February can be seen from Figure 12b. The tendency to increase with height could possibly because of the significant mean vertical shear (not shown) at low levels.

Profile of normalized vertical variances on 9, 10 and 22 February (Fig. 13) on the other hand, appears to be better behaved over the Gulf Stream, the region of strong circulation. Even in the region of strong circulation, the profiles of normalized vertical velocity has one-third maximum. Their vertical variation is close to the AMTEX (Air Mass Transformation Experiments) data reported by Lenschow et al (1980). It is encouraging to note that similarity relations are valid even when a meso-low developed in the region.

4.3. *Vertical variation of the temperature and humidity flux*

Sensible heat flux profiles on 9,10 and 22 February normalized by the near surface values are shown in Fig. 14. The linear line is from AMTEX data (Lenschow et al., 1980). The nor-

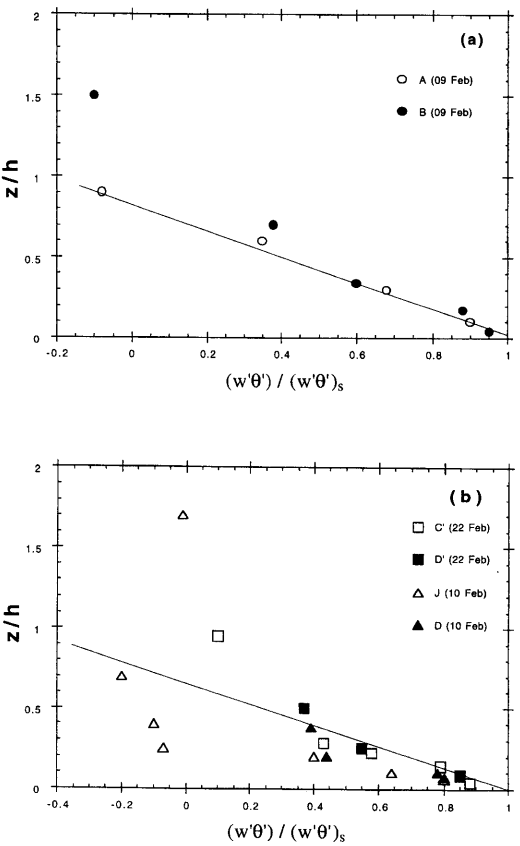

Fig. 14. Vertical profiles of turbulent sensible heat flux normalized by their corresponding surface value on (a) 9 February and (b) 10 and 22 February. Solid diagonal lines are free convection predictions. Locations A, B, J and D are as shown in Fig. 1 and C′ and D′ are as shown in Fig. 3.

malized sensible heat fluxes ($\overline{w'\theta'}$) on 9 February over cold and warm waters (stacks A and B, respectively) are decreasing almost linearly with height and can be described by:

$$\frac{\overline{w'\theta'}}{(\overline{w'\theta'})_0} = 1 - 1.28\,(z/h).$$

This result is in general agreement with the observations during a cold air outbreak on January 28, 1986 (Wayland and Raman, 1989). However, the sensible heat flux profiles on 10 and 22 February (Fig. 14b) did not decrease linearly with height. This could be due to the appreciable horizontal inhomogeneity in the SST field with values varying from 18°C to 25°C in the region of the mesoscale circulation.

The normalized kinematic water vapor fluxes on 9, 10 and 22 February are shown in Fig. 15. The linear line is from AMTEX data (Lenschow et al., 1980) and can be described by:

$$\frac{\overline{w'q'}}{(\overline{w'q'})_0} = 1 - 0.84\,(z/h).$$

Normalized flux values on 9 February (data represented by circles) corresponds to a near linear decrease with height becoming zero near the top of the boundary-layer. However, the profiles of $\overline{w'q'}$ on 10 and 22 February do not decrease linearly with height over the Gulf Stream and over the mid-shelf front. Increase in the values of $\overline{w'q'}$ with height over the Gulf Stream on 10 February could be due to strong advection associated with the development of the offshore mesoscale circulation (Reddy and Raman, 1994).

Thus, normalized temperature and humidity fluxes appear to have decreased linearly with height when conditions are quasi-stationary as on 9 February. But this linear relationship was not observed in a region of strong convergence.

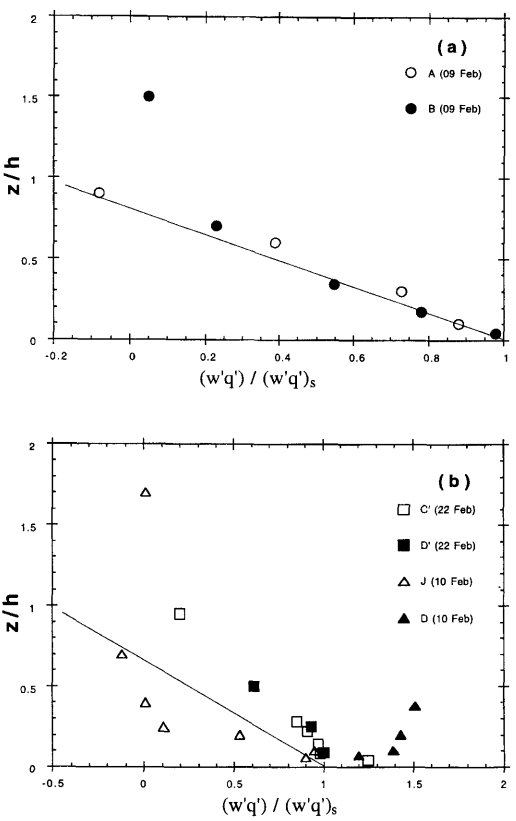

Fig. 15. Vertical profiles of turbulent latent heat fluxes normalized by their corresponding surface value on (a) 9 February and (b) 10 and 22 February. Solid diagonal lines are free convection predictions. Locations A, B, J and D are as shown in Fig. 1 and C′ and D′ are as shown in Fig. 3.

5. Conclusions

Temporal and spatial evolution of the MBL structure during pre-storm conditions on 9 February and a developing meso-low offshore on 10 February are discussed. On 10 February, two low-level convergence zone were present, one near the Gulf Stream and the other close to the coast. These convergence zones were associated with the development of a meso-low. MBL structures at these three distinct mesoscale regions were significantly different. The temperature profiles near the east coast of United States (convergence zone near the coast) indicated stable boundary-layer which could be due to the warm air advection from warmer waters east. Boundary-layer on 9 February was convective and well mixed. But on 10 February, strong shear associated with a low level jet was evident in the mean wind structure.

Temperature and humidity variances during prestorm conditions (9 February) generally followed the free convection relations. But on 10 February with a meso-low, the similarity relations do not appear to be valid for temperature and humidity variances. Normalized sensible heat

fluxes appear to have reasonable similarity relations when conditions are quasi-stationary as on 9 February or strongly convective as on 10 February over the Gulf Stream. But the similarity relations were not satisfactory for sensible heat fluxes in regions of strong convergence. In the region of strong convection (over the Gulf Stream) similarity relations were not satisfactory for moisture fluxes.

7. Acknowledgments

This study was supported by the Division of Atmospheric Sciences, National Science Foundation under grant ATM–92–12636 and by the Department of Energy under contract 091575-A-Q1 with Pacific Northwest Laboratories.

REFERENCES

Anthes, R. A., Kuo, Y.-H. and Gyakum, J. R., 1983. Numerical simulations of a case of explosive cyclogenesis. *Mon. Wea. Rev.* **111**, 1174–1188.

Atlas, R. 1987. The rôle of oceanic fluxes and initial data on the numerical prediction of an intense coastal storm. *Dyn. Atmos. Oceans.* **10**, 359–388.

Bosart, L. F. 1975. New England coastal frontogenesis. *Q. J. R. Meteorol. Soc.* **101**, 000–000.

Bosart, L. F., Vaudo, C. J. and Helsdon, J. H. Jr., 1972. Coastal frontogenesis. *J. Appl. Meteor.* **11**, 1236–1258.

Bosart, L. F. 1981. The President's Day snowstorm of 18–19 February 1979: A sub-synoptic scale event. *Mon. Wea. Rev.* **107**, 1542–1566.

Chou, S. H., Atlas, D. and Yeh, E.-N. 1986. Turbulence in a Convective Marine Atmospheric boundary-layer, *J. Atmos. Sci.* **43**, 547–564.

Dirks, R. A., Kuettner, J. P. and Moore, J. A. 1988. Genesis of Atlantic Lows Experiment (GALE). An overview, *Bull. Amer. Meteorol. Soc.* **69**, 148–160.

Friehe, C. A. and Schmitt, K. F. 1976. Parameterization of air-sea interface fluxes of sensible heat and moisture by the bulk aerodynamic formulas. *J. Phys. Oceanogr.* **6**, 801–809.

Holt, T. and Raman, S. 1990. Marine Boundary-layer Structure and Circulation in the Region of offshore Redevelopment of a Cyclone during GALE. *Mon. Wea. Rev.* **118**, 382–410.

Holt, T. and Raman, S. 1992. Three-dimensional mean and turbulence structure of a coastal front influenced by the Gulf Stream. *Mon. Wea. Rev.* **120**, 17–39.

Kocin, P. J. and Uccellini, L. W. 1985a. A survey of major east coast snow storms, 1960–1983. Part I: Summary of surface and upper level characteristics. NASA TM 86195, 101pp (NTIS N85–2747; tentatively accepted for publication as a meteorological monograph).

Kocin, P. J. and Uccellini, L. W. 1985b. A survey of major east coast snow storms, 1960–1983. Part II: Case studies of eighteen storms. NASA TM 86196, 214pp (NTIS N85–27472; tentatively accepted for publication as a meteorological monograph).

Kuo, Y.-H., Reed R. J. and Simon, L.-N. 1991. Effects of surface energy fluxes during the early development and rapid intensification stages of seven explosive cyclones in the western Atlantic. *Mon. Wea. Rev.* **119**, 457–476.

Lenschow, D. H., Wyngaard J. C. and Pennell, W. T. 1980. Mean-field and second-moment budgets in a baroclinic, convective boundary-layer. *J. Atmos. Sci.* **37**, 1313–1326

Raman, S., Riordan, A. J., Holt, T., Stunder, M. and Hinman, J. 1986. Observations of the marine boundary-layer thermal structure over the Gulf Stream during a cold-air outbreak. *J. Appl. Clim. Meteorol.* **25**, 14–21.

Raman, S. and Riordan, A. J. 1988. The genesis of Atlantic lows experiment: The planetary boundary-layer subprogram. *Bull. Amer. Meteoro. Soc.* **69**, 161–172.

Reddy, N. C and Raman, S. 1994. Observations of a mesoscale circulation over the Gulf Stream region. *The Glo. Atmos. and Ocean Sys.* **2**, 21–39.

Riordan, A. J. 1990. Examination of the mesoscale features of the GALE coastal front of 24–25 January 1986. *Mon. Wea. Rev.* **118**, 258–282.

Rogers, D. P. 1989. The marine boundary-layer in the vicinity of an ocean front. *J. Atmos. Sci.* **46**, 2044–2062.

Sanders, F. and Gyakum, J. R. 1980. Synoptic-dynamic climatology of the bomb. *Mon. Wea. Rev.* **108**, 1589–1606.

Sanders, F. 1986. Explosive cyclogenesis in the west-central North Atlantic ocean, 1981–1984. Part I. Composite structure and man behavior. *Mon. Wea. Rev.* **114**, 1781–1794.

Uccellini, L. W., Petersen, R. A., Brill, K. F., Kocin, P. J. and Tucillo, J. J. 1987. Synergistic interaction between an upper-level jet streak and diabatic processes that influence of the development of a low level jet and a secondary coastal cyclone. *Mon. Wea. Rev.* **115**, 2222–2261.

Warner, T. T., Lakhatia, M. N., Doyle J. D. and Pearson, R. A. 1990. Marine atmospheric boundary-layer circulations forced by the Gulf Stream sea surface temperature gradients. *Mon. Wea. Rev.* **118**, 309–323.

Wayland, R. J. and Raman, S. 1989. Mean and turbulent structure of a baroclinic marine boundary-layer during the 28 January 1986 Cold-air outbreak (GALE 86). *Boundary-Layer Meteo.* **48**, 227–254.

Wyngaard, J. C., Cote O. R. and Izumi, Y. 1971. Local free convection, similarity and the budgets of shear stress and heat flux. *J. Atmos. Sci.* **28**, 1171–1182.